Organic & Biomolecular Chemistry

Dynamic Article Links

Cite this: *Org. Biomol. Chem.*, 2011, **9**, 5476

www.rsc.org/obc

PAPER

Flustramine inspired synthesis and biological evaluation of pyrroloindoline triazole amides as novel inhibitors of bacterial biofilms†

Cynthia Bunders,[a] John Cavanagh[b] and Christian Melander*[a]

Received 14th April 2011, Accepted 17th May 2011
DOI: 10.1039/c1ob05605k

Anti-biofilm agents have been developed based upon the flustramine family of alkaloids isolated from *Flustra foliacea*. A Garg interrupted Fischer indolization reaction was employed to access a core pyrroloindoline scaffold that was subsequently employed to create a pyrroloindoline triazole amide library. Screening for the ability to modulate biofilm formation against strains of Gram-positive and Gram-negative bacteria identified several compounds with low micromolar, non-toxic IC_{50} values.

Biofilms are populations of microorganisms that exist as an organized community. They can be found in any environment in which bacteria, moisture, nutrients, and a surface for attachment are present. Biofilms are advantageous to bacteria because they provide individual cells with shelter, food, and diversity, all of which allow the bacteria to survive environmental selection pressures.[1] The National Institute of Health (NIH) estimates that over 75% of microbial infections that occur in the human body are linked to the formation of biofilms. Some common diseases associated with the formation of biofilms are: lung infections in cystic fibrosis (CF) patients, burn wounds, gastrointestinal infections, urinary tract infections, and dental plaque.[1,2] There is an immense need for innovative solutions to combat bacterial biofilms, as conventional methods such as antiseptics, antibiotics, and other antimicrobials are becoming increasingly ineffective.[3]

One approach to the discovery of anti-biofilm agents is through the use of natural products as structural inspiration for analogue design. Emboldened by our success with the 2-aminoimidazole scaffold diverged from oroidin/ageliferin and the ethyl *N*-(2-phenyl) carbamate scaffold, we have begun to explore the potential of the indole derived flustramine family of natural products to serve as scaffolds for analogue design and to ultimately probe bacterial biofilm modulation (Fig. 1).[4] The flustramine family is a collection of monobrominated alkaloids that contain a pyrroloindoline or indolic core. These secondary metabolites were isolated from *Flustra foliacea*, a marine invertebrate, found in the North Bryozoan Sea.[5]

A major defining feature of the flustramine family is that it possesses several members that have interesting biological activity,

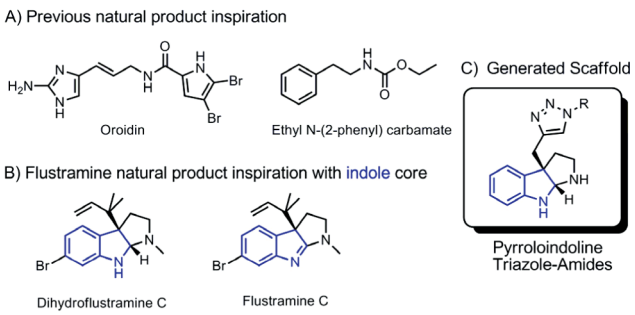

Fig. 1 A) Marine alkaloid natural product inspiration in the Melander lab. B) Two of the most biologically active flustramine analogues. C) Designed scaffold incorporating flustramine inspiration and allowing for facile generation of analogues.

including the ability to eradicate bacteria native to the environment they inhabit.[6] It has also been reported that dihydroflustramine C inhibits production of reporter genes in an acyl homoserine lactone (AHL)-based quorum sensing reporter assay (IC_{50} 20 μg mL^{-1} or 62 μM), and is thus hypothesized to inhibit AHL-driven gene transcription.[6] This suggests that this class of natural products might have the ability to control quorum sensing. Given that quorum sensing and biofilm formation have an undoubted connection to one another, we envisioned that small molecules based on the flustramine scaffolds might serve as potential candidates to inhibit the formation of Gram-negative and Gram-positive biofilms.[7]

The second determining factor that stimulated the selection of the flustramine scaffold was that indole itself has been established as an ubiquitous intercellular signal, and is produced by both Gram-negative and Gram-positive bacteria.[8] Indole has demonstrated the ability to control numerous phenotypes in bacteria, such as drug resistance, biofilm formation, virulence, and the ability to alter phenotypes of other bacteria that do not produce indole.[9] Most recently, studies demonstrate that the concentration of indole produced by *Escherichia coli* is dependent on pH and temperature, and correspondingly determines the quantity of

[a]*Department of Chemistry, North Carolina State University, Raleigh, North Carolina, 27695, USA. E-mail: Christian_Melander@ncsu.edu; Fax: +1 919-515-5079; Tel: +1 919-513-2960*
[b]*Department of Molecular and Structural Biochemistry, North Carolina State University, Raleigh, North Carolina, 27695, USA. E-mail: john_cavanagh@ncsu.edu*

† Electronic supplementary information (ESI) available: ^{1}H and $^{13}CNMR$, ESI-MS, UV-Vis, IR, biofilm inhibition, and growth curves analyses. See DOI: 10.1039/c1ob05605k

biofilm formation.[9,10] Therefore, it appears that indole signalling is widespread and could be present among a majority of the microbial community, and we thus posited that the flustramine family, containing a deep-seated indole core, may lead us to small molecules that have the ability to regulate bacterial biofilms and ultimately deliver small molecule probes to dissect indole signalling *in vitro* and *in vivo*.

To test the potential of the flustramine family to serve as a template for the design of anti-biofilm compounds, we synthesized flustramine C[11] and evaluated its activity against three strains of bacterial pathogens: *Acinetobacter baumannii*, *E. coli*, and methicillin resistant *Staphylococcus aureus* (MRSA). *A. baumannii*, a Gram-negative bacterium that forms robust films, was selected for this study because of its rising prominence in hospital acquired infections, especially those of military personnel in Iraq and Afghanistan.[12] This bacterium is difficult to eradicate and has been found to have survived for weeks on surfaces, making it hard to disinfect hospital and medical equipment. MRSA, a Gram-positive bacterium that is resistant to numerous antibiotics was investigated because it has emerged as a serious health problem for patients with immunocompromised systems.[13] *E. coli*, a Gram-negative bacterium, is commonly found in the lower intestines of warm-blooded organisms. Most *E. coli* strains are harmless, but some can cause serious food poisoning (*i.e.* enterotoxigenic *E. coli* (ETEC) aka travellers' diarrhea). It has been reported that an estimated 280 million episodes of ETEC diarrhea occur each year in children under five in developing countries, with 20% of these cases leading to death.[14] To our delight we observed moderate biofilm inhibition activity against *A. baumannii* (30% at 100 μM) with flustramine C.

Based on this initial result we then began to analyze the components of flustramine C to determine where modification could be made to rapidly create a library of analogues for further screening. In our experience with the 2-aminoimdazole scaffold, we have noted that the most active biofilm inhibitors tend to be amphipathic. Based on this observation we elected to keep the aminal construct and modulate the identity of the reverse prenyl group with an alkyne, which could be further elaborated through click chemistry to introduce different hydrophobic components *via* a triazole amide moiety (Fig. 1). Herein we describe the synthesis and anti-biofilm activity of pyrroloindoline-triazole-amide (PTA) analogues based on the flustramine family. These small molecules were tested against the three above mentioned medically relevant strains of bacteria (*A. baumannii*, *E. coli*, and MRSA) with the aim of identifying molecules that inhibit bacterial biofilm formation efficiently.

To access the alkyne derived flustramine derivative as a base scaffold for analogue design, we elected to employ Garg's interrupted Fischer indolization methodology.[15] Our first attempt to produce flustramine analogues centered on synthesizing bromopyrroloindoline **1**. This scaffold contains similar components to those in flustramine A–E and it was envisioned that 3-bromophenylhydrazine could be employed in the indolization step to produce analogues with bromine at the six position. It was quickly determined however, that we would have to produce debromo analogues, as the interrupted Fischer indolization reaction of 3-bromophenylhydrazine with key intermediate **5** was unsuccessful despite numerous attempts and modifications to the procedure.

Our approach to the key des-bromo pyrroloindoline **6** is outlined in Scheme 1. The protected lactam **3** was synthesized with a slight modification to Garg's synthesis in that the toluenesulfonyl (Ts) group was exchanged for an *o*-nitrobenzenesulfonyl (Ns) protecting group. We found that in our system the Ts group was difficult to remove at the end of the synthesis to generate deprotected analogues for screening. The Ns group allowed for the use of Fukuyama's deprotection conditions which utilized thiophenol, potassium carbonate, and CH_3CN at room temperature to provide the tricyclic aminal core in a facile way with high yield (Scheme 2).[16] The protected lactam **3** was alkylated with propargyl bromide to give **4**. The reduction of the protected lactam to the hemiaminal **5** proceeded efficiently under standard DIBAL-H conditions. The Fischer indolization reaction was then carried out utilizing microwave irradiation to provide a more time efficient reaction. The conditions employed in our synthesis were 5 min at 150 °C opposed to 1.5 h at 100 °C for conventional heating, forming the tricyclic core **6** in 52% yield as originally reported by Garg.[15]

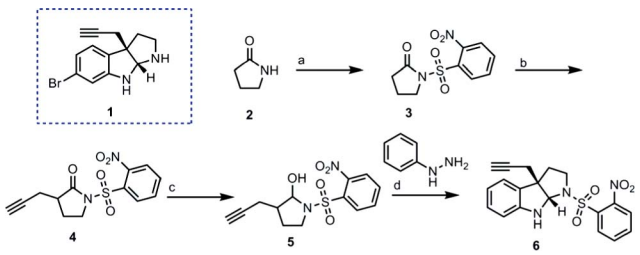

Scheme 1 Desired scaffold **1** based on flustramine family, and synthesis of intermediate **6**. Reagents and conditions: (a) i) BuLi, THF ii) *o*-nitrobenzenesulfonylchloride, THF, −78 °C; (b) i) BuLi, hexamethyldisilazane, THF ii) propargylbromide, THF, −78 °C; (c) DIBAL-H, CH_2Cl_2, −78 °C; (d) AcOH : H_2O (1 : 1), 150 °C μwave, 5 min.

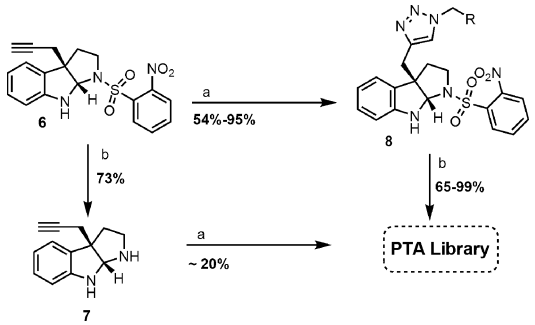

Scheme 2 Click and deprotection conditions: (a) $CuSO_4 \cdot 5H_2O$, sodium ascorbate, azide, CH_2Cl_2, EtOH, H_2O, rt (b) PhSH, K_2CO_3, CH_3CN, rt.

With the core formed we then determined the optimal sequence of alkyne functionalization and protecting group removal (Scheme 2). Initially, we performed the deprotection step first. This method provided a 73% yield of the tricyclic aminal alkyne intermediate **7**. From this intermediate, three derivatives were synthesized *via* the click reaction; however these analogues were accessed in poor yield (~ 20%). Since the click reaction with this alkyne was low yielding, we contemplated that it might be beneficial to form the triazole (**8**) first then perform the

deprotection to afford the desired products. This route improved yields to 54–96% yield for the click reaction and 65–98% for the deprotection step (Fig. 2). Although this route involved more synthetic steps it provided the desired compounds in higher yields. The synthesis proceeded with the use of an array of readily available azide-amides (Fig. 2).[17]

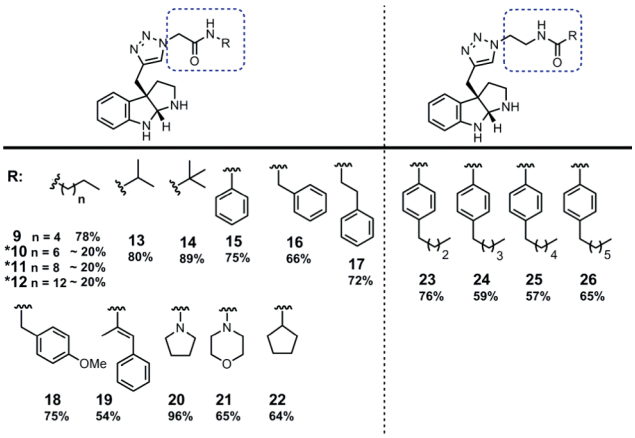

Fig. 2 18 member pyrroloindoline trizaole amide library with corresponding click reaction yields. * = click yield with deprotected intermediate **7**.

Biological screening

The evaluation of the PTA library commenced with screening each small molecule for biofilm inhibition activity at 200 μM against *A. baumannii*, *E. coli*, and MRSA. The activity of each molecule was then assessed and dose response curves were obtained for active analogues. Active molecules were also evaluated for their toxicity to planktonic bacteria using growth curve and colony count analysis. These experiments confirm whether the active small molecule is simply killing planktonic bacteria, or modulating biofilm formation through a non-microbicidal mechanism. From our 18 compound library, two moieties emerged and were identified as most active: analogues with aliphatic chains (Table 1) and alkyl phenyl moieties (Table 2).

Against *E. coli*, compound **11** exhibited the lowest non-toxic IC_{50} (35.7 μM). For this strain of Gram-negative bacteria the PTA library illustrated that maximum activity is elicited with a decyl aliphatic chain. Molecules **23–26** exhibited moderate activity against *E. coli* with only compound **26** being active (IC_{50} 71.0 μM);

Table 1 IC_{50} values and percentage inhibition of compounds **9–12** and **19**

Compound	IC_{50}(μM) *E. coli*	IC_{50}(μM) *A. baumannii*	IC_{50}(μM) MRSA
9	30% @ 200	25% @ 200	< 5% @ 200
10	147.5 ± 4.0	192.5 ± 5.0	86.0 ± 5.0
11	35.7 ± 2.5	125.2 ± 4.5[a]	25.0 ± 2.0[a]
12	103.7 ± 5.0	40% @ 200	5.4 ± 1.0[a]
19	< 5% @ 200	< 5% @ 200	78.0 ± 3.0

[a] Indicates inhibition of biofilm formation through a toxic mechanism as determined by growth curve analysis.

Table 2 IC_{50} and percentage inhibition of compounds **23–26**

Compound	IC_{50}(μM) *E. coli*	IC_{50}(μM) *A. baumannii*	IC_{50}(μM) MRSA	IC_{50}(μM) *S. aureus*
23	20% @ 200	40% @ 200	13.5 ± 1.5	< 5% @ 200
24	167.0 ± 2.0	206.4 ± 5.0	6.6 ± 0.8	33.3 ± 1.8
25	100.0 ± 2.0[a]	90.0 ± 5.0[a]	3.4 ± 1.0	12.5 ± 1.3[a]
26	71.0 ± 5.0[a]	20.0 ± 2.0[b]	2.8 ± 1.0[a]	6.6 ± 1.9.[a]

[a] Indicates inhibition of biofilm formation through a toxic mechanism determined by growth curve analysis. [b] Indicates not complete toxicity, bacterial growth delay is noted in the first 8 h, bacterial density is identical at 24 h.

however this compound was determined to be toxic to planktonic bacteria at this concentration.

When the library was screened against *A. baumannii* only compounds **10** and **24** (IC_{50} = 192.5 μM and 206.4 μM respectively) were able to efficiently inhibit *A. baumannii* bacterial biofilm formation *via* a non-toxic mechanism. The lowest toxic IC_{50} value determined was for compound **26** (IC_{50} = 20.0 μM). A number of compounds were determined to affect the bacterial growth curve (and are labeled as toxic).

Compounds **10** and **19** displayed moderate activity against MRSA biofilm formation (IC_{50} 78.0 μM, and 86.0 μM respectively). The trend determined for compounds **9–12** against MRSA revealed that increasing chain length augmented potency; however the molecules also became toxic to planktonic bacterial growth. Specifically, we noted that compounds **11** and **12** displayed low micromolar IC_{50} values (25.0 μM and 5.4 μM respectively) but were toxic to planktonic bacteria. Thus to generate non-toxic PTA analogues against MRSA, the aliphatic appendage should not exceed eight carbon units.

Compounds (**23–25**) that contained alkyl-derivatized-phenyl rings also demonstrated exceptional non-toxic activity against MRSA (Table 2), exhibiting IC_{50} values of 13.5 μM, 6.6 μM, and 3.4 μM respectively. PTA analogue **26** displayed more potent activity but was determined to affect early bacterial growth at its IC_{50} concentration (2.8 μM); however we noted that after 24 h bacterial density is identical to the untreated control. As we observed for the aliphatic analogues **9–12**, the potency of compounds **23–26** increased as a function of chain length, however *para*-substituents longer than hexyl affected bacterial growth.

Due to the exceptional activity of compounds **23–26** against MRSA we envisioned that these compounds might have the capability to affect the biofilm formation of other strains of *Staphylococcus aureus*, a bacterium that is the leading cause of bacterial infections worldwide. To our delight, three of the four molecules efficiently inhibited biofilm formation by a methicillin sensitive strain of *S. aureus*, with IC_{50} values correlating to the chain length of the 4-alkylphenyl appendage (Fig. 3). Compounds **24**, **25**, and **26** exhibited IC_{50} values of 32.0 μM, 12.5 μM, and 6.6 μM respectively; however, only compound **24** inhibited *S. aureus* biofilm formation *via* a non-toxic mechanism.

To further investigate structural components within the PTA scaffold that drive biofilm inhibition, we exploited the interrupted Fischer indolization reaction to access an alkyne furindoline core **29** (Scheme 3).[15] We utilized Garg's methodology to access

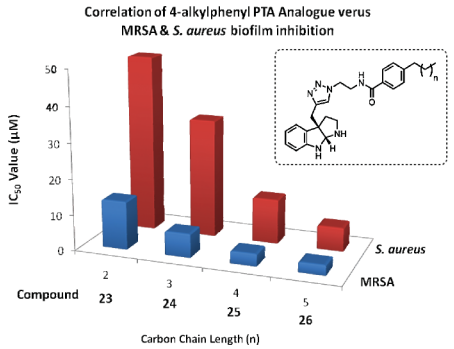

Fig. 3 Correlation of 4-alkylphenyl PTA chain length and inhibition of Gram-positive bacterial biofilm formation. Compound **23** ($n = 2$) for *S. aureus* was not active at any tested concentrations but the graph is capped at 50 μM, to show the relationship among the analogues.

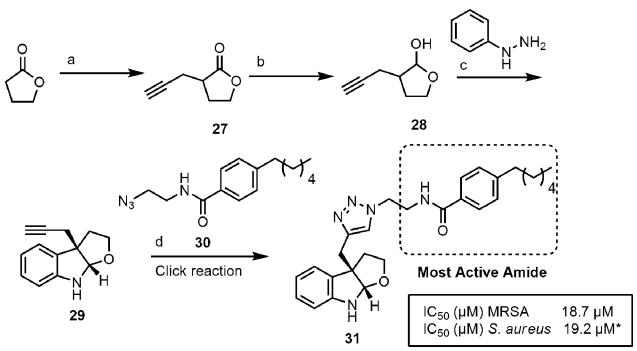

Scheme 3 Synthesis of furindoline **31**. IC_{50} values of compound **31**.* = Indicates inhibition of biofilm formation through a toxic mechanism as determined by growth curve analysis. Reagents and conditions: (a) i) BuLi, hexamethyldisilazane, THF ii) propargylbromide, THF, −78 °C; (b) DIBAL-H, CH_2Cl_2, −78 °C; (c) AcOH : H_2O (1 : 1), 60 °C, 4.5 h; (d) $CuSO_4 \cdot 5H_2O$, sodium ascorbate, azide 30, CH_2Cl_2, EtOH, H_2O, rt.

intermediate **27**, which was then reduced to hemiacetal **28** and cyclized to provide us with the furindoline core **29**. Next, through the click reaction, we reacted **29** with azide amide **30** to afford furindoline **31**, our targeted analogue of compound **25** (IC_{50} value of 3.4 μM against MRSA). To evaluate the effects of this substitution we screened **31** for biofilm inhibition activity against MRSA and. *S. aureus.* The furindoline core proved to be less active as an inhibitor of both strains compared to its pyrroloindoline analogue, but did exhibit IC_{50} values of 18.7 μM and 19.2 μM for MRSA and *S. aureus* respectively. By replacing the nitrogen in our heterocyclic core with oxygen there is a 5.5 fold decrease in MRSA activity and a 1.6 fold decrease in *S. aureus* activity (Scheme 3). Similar to analogue **25**, compound **31** inhibited the Gram-positive bacterial biofilms in a non-toxic manner for MRSA and through a toxic mechanism for *S. aureus*.

To further decipher which functionality of the PTA library was most critical for biological activity we synthesized two control compounds (**32** and **33**). A one step click reaction between propargyl amine and an azide amide produced the target control compounds (Table 3). These compounds were examined for anti-biofilm activity, along with intermediates **6** and **7** (which contain only the tricyclic core). All control compounds were inactive

Table 3 Biological evaluation of control triazole analogues **32** and **33** and intermediates **6** and **7** at 200 μM. Flustramine C, structural inspiration, was screened at 150 μM. Compound **25**, our lead PTA analogue, is shown for comparison purposes

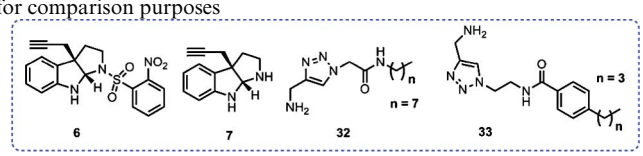

Compound	*E. coli* biofilm inhibition	*A. baumannii* biofilm inhibition	MRSA biofilm inhibition
6	<5%	<5%	<5%
7	<5%	<5%	<5%
32	<5%	<5%	<5%
33	30%	<5%	15%
Flustramine C	30%	20%	< 5%
25	90.0 μM[a]	100.0 μM[a]	3.4 μM

[a] Indicates inhibition of biofilm formation through a toxic mechanism determined by growth curve analysis.

leading us to posit that both segments of the molecule are critical for biological activity. Table 3 also includes flustramine C and our lead PTA analogue **25** to reinforce that the tail or hydrophobic region and substitution on the heterocycle are indeed critical to a small molecule's ability to inhibit bacterial biofilms.

Conclusions

In conclusion, we have accessed pyrroloindoline triazole amides through an interrupted Fischer indolization reaction. Using this approach, a set of 18 tricyclic indole derivatives with a wide variety of functionality introduced through a click reaction was screened against *A. baumannii*, *E. coli*, and MRSA. A structure activity relationship was observed for compounds **23–26** based on the chain length of the phenyl alkyl appendage and these compounds exhibited low micromolar non-toxic IC_{50} values against two strains of Gram-positive bacteria. We also note that some of the compounds with long alkyl chains are also potent biofilm inhibitors; however they do so *via* a toxic mechanism. This is potentially due to compounds forming channels within the bacterial cell wall. A furindoline analogue **31** was synthesized containing the most active amide appendage, and was determined to be a less active inhibitor of *S. aureus* and MRSA biofilm formation in comparison to the pyrroloindoline analogue **25**. This indicated that the secondary nitrogen enhances activity presumably through additional H-bond donor interactions with its biological target or altered cell uptake properties. These PTA analogues may serve as probes to potentially deconvolute bacterial signalling pathways both *in vitro* and *in vivo*. Investigation of the most active PTA analogues may probe the intriguing question of whether this class of compounds can specifically block interactions that lead to disease causing phenotypes and production of virulence factors, in addition to biofilm formation. The PTA scaffold also contains numerous synthetic handles that can be manipulated and further optimized to generate more advanced analogues with enhanced activity.

Experimental

Synthesis

All reagents used for chemical synthesis were purchased from commercially available sources and used without further purification. Chromatography was performed using 60-mesh standard silica gel from Sorbtech. NMR solvents were obtained from Cambridge Isotope Labs and were used as is. ^{1}H NMR (300 MHz or 400 MHz) and ^{13}C NMR (75 MHz or 100 MHz) spectra were recorded at 25 °C on Varian Mercury spectrometers. Chemical shifts (δ) are given in ppm relative to the respective NMR solvents; coupling constants (J) are in hertz (Hz). Abbreviations used are s = singlet, bs = broad singlet, d = doublet, dd = doublet of doublets, t = triplet, td = triplet of doublets, m = multiplet, d_{ab} = ab doublet, dd_{ab} = ab doublet of doublet. Mass spectra were obtained at the NCSU Department of Chemistry Mass Spectrometry Facility. Infrared spectra were obtained on a FT/IR-4100 spectrophotometer (ν_{max}/cm^{-1}). UV absorbance was recorded on a Genesys 10 scanning UV/visible spectrophotometer (λ_{max} = nm).

General procedure for the preparation of intermediate 6

Hemiaminal **5** (250 mg, 0.805 mmol) was reacted with similar synthetic methods developed by Garg[15] with slight modification. Microwave heating at 150 °C for five minutes was used opposed to conventional heating. Purification by flash chromatography (10–30% EtOAc : Hexanes) afforded **6** as an orange foam (160 mg, 52% yield). ^{1}H NMR (300 MHz, $CDCl_3$) δ 8.04–8.01 (m, 1H), 7.73–7.64 (m, 3H), 7.17–7.10 (m, 2H), 6.79 (td, 1H, J = 7.5 Hz, J = 0.9 Hz), 6.63 (dd, 1H, J = 8.4 Hz, J = 0.6 Hz), 5.50 (s, 1H), 5.00 (s, 1H (NH)), 3.68 (td, 1H, J = 7.8 Hz, J = 1.2 Hz), 3.27–3.18 (m, 1H), 2.59 (dd_{ab}, 2H, J = 7.8 Hz, J = 1.2 Hz), 2.48–2.40 (m, 1H), 2.92–2.30 (m, 1H), 1.92 (t, 1H, J = 2.7 Hz). ^{13}C NMR (75 MHz, $CDCl_3$) δ 202.2, 148.7, 133.8, 133.2, 131.9, 130.7, 130.2, 129.4, 124.5, 123.3, 119.6, 109.7, 82.6, 80.3, 70.8, 57.4, 48.0, 35.7, 27.6; HRMS (ESI) calcd for $C_{19}H_{18}N_3O_4S$ (M^+)+ 384.1013, found 384.1010; IR ν_{max}/cm^{-1} 3405, 3287, 2916, 2364, 1616, 1539, 1462, 1357, 1168, 1056, 735; λ_{max}: 226 nm, 280 nm.

General procedure for click reaction

Intermediate **6** (36 mg, 0.093 mmol) was dissolved in 1 : 1 ethanol–water (2 mL total) and placed in a vial. Azide **30** (26 mg, 0.093 mmol) was then dissolved in dichloromethane (1 mL) and added to the reaction vial. Next sodium ascorbate (11 mg, 0.056 mmol) and copper sulfate (5 mg, 0.028 mmol) were added to the reaction vial. The reaction mixture was then stirred for 16 h. The crude reaction was quenched with water (5 mL) and diluted with EtOAc (5 ml). The organic layer was washed with water (3 × 5–10 mL), dried over Na_2SO_4, and concentrated with reduced pressure to afford the crude product, which was then purified by flash chromatography (1–5% MeOH–CH_2Cl_2) afforded **25a** as a yellow foam (57% yield).^{1}H NMR (400 MHz, $CDCl_3$) δ 8.00–7.96 (m, 1H), 7.70–7.62 (m, 3H), 7.62–7.60 (m, 1H), 7.23 (s, 1H) 7.04 (td, 2H, J = 7.6 Hz, J = 1.2 Hz), 7.02 (s, 1H), 6.96 (d, 2H, J = 7.2 Hz), 6.76 (t, 1H, J = 6.0 Hz), 6.72 (td, 1H, J = 7.2 Hz, J = 1.2 Hz), 6.45 (d, 1H, J = 8.0 Hz) 5.48 (s, 1H), 4.82 (s, 1H), 4.56–4.48 (m, 2H), 3.88–3.83 (m, 2H), 3.49–3.42 (m, 1H), 3.20–3.04 (m, 3H), 2.64 (t, 2H, J = 7.6 Hz), 2.40–2.37 (m, 1H), 2.25–2.20 (m, 1H), 1.65–1.56 (m, 2H), 1.29–1.23 (m, 6H), 0.87 (t, 3H, J = 7.6 Hz). ^{13}C NMR (100 MHz, $CDCl_3$) δ 167.7, 148.9, 147.7, 147.6, 143.5, 133.9, 133.6, 132.2, 131.2, 131.0, 130.0 129.2, 128.9, 127.3, 124.5, 123.4, 123.1, 119.5, 109.5, 82.2, 58.4, 49.7, 47.5, 40.2, 36.6, 36.1, 33.8, 31.9, 31.4, 29.2, 22.8, 14.3; HRMS (ESI) calcd for $C_{34}H_{40}N_7O_5S$ (M+H)+ 658.2806, found 658.2807; IR ν_{max}/cm^{-1} 3398, 2921, 2859, 1644, 1539, 1166; λ_{max}: 236 nm, 282 nm.

General procedure for deprotection

25a (35 mg, 0.096 mmol) was placed in a vial and dissolved in 4 mL of CH_3CN. Then K_2CO_3 (53 mg, 0.386 mmol) was added to the vial, then thiophenol (21.0 mg, 0.193 mmol) was added dropwise and the reaction was stirred for 16 h at room temperature. The reaction was then concentrated under reduced pressure to afford crude aminal **25**, which was purified by flash chromatography (1–5% sat. NH_3–MeOH–CH_2Cl_2) to afford **25** as an oil (66% yield). ^{1}H NMR (300 MHz, $CDCl_3$) δ 7.62 (d, 2H, J = 8.4 Hz), 7.23 (d, 2H, J = 8.4 Hz), 7.00–6.92 (m, 2H), 6.72 (s, 1H), 6.64 (td, 1H, J = 7.2 Hz, J = 1.2 Hz), 6.54 (t, 1H, J = 6.0 Hz), 6.32 (d, 1H, J = 7.5 Hz), 4.97 (s, 1H), 4.47–4.40 (m, 2H), 3.86–3.78 (m, 2H), 3.21 (d_{ab}, 2H, J = 14.4 Hz), 3.00–2.94 (m, 1H), 2.74–2.687 (m, 1H), 2.64 (t, 1H, J = 7.8 Hz), 2.14–2.08 (m, 1H), 2.00–1.90 (m, 1H), 1.61–1.55 (m, 2H), 1.30–1.25 (m, 6H), 0.87 (t, 3H, J = 7.2 Hz). ^{13}C NMR (75 MHz, $CDCl_3$) δ 168.0, 151.1, 147.6, 145.2, 133.1, 131.3, 128.9, 128.5, 127.2, 123.7, 122.8, 118.8, 108.7, 82.2, 58.5, 49.7, 46.1, 41.8, 40.0, 36.1, 35.5, 31.9, 31.4, 29.1, 22.8, 14.3; HRMS (ESI) calcd for $C_{28}H_{37}N_6O$ (M+H)+ 473.3023, found 473.3027; IR ν_{max}/cm^{-1} 3384, 2923, 2853, 1644, 1609, 1546, 1455, 749; λ_{max}: 238 nm, 296 nm.

Acknowledgements

The authors would like to thank the National Institute of Health (GM055769 to JC and CM) for support of this work.

Notes and references

1 D. Musk and P. Hergenrother, *Curr. Med. Chem.*, 2006, **13**, 2163; J. J. Richards and C. Melander, *ChemBioChem*, 2009, **10**, 2287.
2 P. Singh, A. L. Schaefer, M. R. Parsek, T. O. Moninger, M. Welsh and E. P. Greenberg, *Nature*, 2000, **407**, 762.
3 L. Hall-Stoodley, W. J. Costerton and P. Stoodley, *Nat. Rev. Microbiol.*, 2004, **2**, 95; J. W. Costerton, P. S. Stewart and E. P. Greenberg, *Science*, 1999, **284**, 1318.
4 E. T. Ballard, J. J. Richards, A. Aquino, C. S. Reed and C. Melander, *J. Org. Chem.*, 2009, **74**, 1755; E. T. Ballard, J. J. Richards, A. L. Wolfe and C. Melander, *Chem.–Eur. J.*, 2008, **14**, 10745; S. A. Rogers, D. C. Whitehead, T. Mullikin and C. Melander, *Org. Biomol. Chem.*, 2010, **8**, 3857; S. A. Rogers, E. A. Lindsey, D. C. Whitehead, T. Mullikin and C. Melander, *Bioorg. Med. Chem. Lett.*, 2011, **21**, 1257.
5 J. S. Carle and C. Christopherson, *J. Am. Chem. Soc.*, 1979, **101**, 4012; J. S. Carle and C. Christopherson, *J. Org. Chem.*, 1980, **45**, 1586; J. S. Carle and C. Christopherson, *J. Org. Chem.*, 1981, **46**, 3440.
6 L. Peters, G. Ko, A. D. Wright, R. Pukall, E. Stackebrandt, L. Eberl and K. Riedel, *Appl. Environ. Microbiol.*, 2003, **69**, 3469.
7 A. Jayaraman and T. K. Wood, *Annu. Rev. Biomed. Eng.*, 2008, **10**, 14.
8 J. H. Lee and J. Lee, *FEMS Microbiol. Rev.*, 2010, **34**, 426.
9 J. Lee, A. Jayaraman and T. K. Wood, *BMC Microbiol.*, 2007, **7**, 42; J. Lee, C. Attila, S. L. Cirillo, J. D. Cirillo and T. K. Wood, *Microb. Biotechnol.*, 2009, **2**, 75; J. Lee, S. Zhang, M. Hegde, W. E. Bentley, A. Jayaraman and T. K. Wood, *ISME J.*, 2008, **2**, 1007.
10 H. T. Han, J-H. Lee, M. H. Cho, T. K. Wood and L. Lee, *Res. Microbiol.*, 2011, **162**, 108.

11 T. Lindel, L. Brauchle, G. Golz and P. Bohrer, *Org. Lett.*, 2007, **9**, 238.
12 K. A. Davis, K. A. Moran, K. C. McAllister and P. J. Gray, *Emerg. Infect. Dis.*, 2005, **11**, 1218.
13 A. March, A. Aschbacher, H. Dhanji, D. Livermore, A. Böttcher, F. Sleghel, S. Maggi, M. Noale, C. Larcher and N. Woodford, *Clin. Microbiol. Infect.*, 2010, **16**, 934.
14 J. Ouyang-Latimer, N. Ajami, Z. Jiang, P. Okhuysen, M. Paredes, J. Flores and H. DuPont, *J. Infect. Dis.*, 2010, **201**, 1831.
15 B. Boal, A. Schammel and N. Garg, *Org. Lett.*, 2009, **11**, 3458; A. Schammel, B. Boal, L. Zu, M. Tehetene and N. Garg, *Tetrahedron*, 2010, **66**, 4867.
16 T. Fukuyama, C. Jow and M. Cheung, *Tetrahedron Lett.*, 1995, **36**, 6373; C Guisando, J. Waterhouse, W. Price, M. Jorgensen and A. Miller, *Org. Biomol. Chem.*, 2005, **3**, 1049.
17 C. Reed, R. W. Huigens, S. A. Rogers and C. Melander, *Bioorg. Med. Chem. Lett.*, 2010, **20**, 6310.